BMC Pulmonary Medicine

RESEARCH

Open Access

Cepharanthine attenuates pulmonary fibrosis via modulating macrophage M2 polarization

Jiaqi Bao[1,2,3†], Chang Liu[1,2,3†], Huafeng Song[4†], Zheying Mao[1,2,3], Wenxin Qu[1,2,3], Fei Yu[1,2,3], Yifei Shen[1,2,3], Jingjing Jiang[1,2,3], Xiao Chen[1,2,3], Ruonan Wang[1,2,3], Qi Wang[1,2,3], Weizhen Chen[1,2,3], Shufa Zheng[1,2,3*†] and Yu Chen[1,2,3*†]

Abstract

Background Idiopathic pulmonary fibrosis (IPF) is a group of chronic interstitial pulmonary diseases characterized by myofibroblast proliferation and extracellular matrix (ECM) deposition. However, current treatments are not satisfactory. Therefore, more effective therapies need to be explored. Cepharanthine (CEP) is a naturally occurring alkaloid that has recently been reported to have multiple pharmacological effects, particularly in chronic inflammation.

Methods For in vivo experiments, first, a pulmonary fibrosis murine model was generated via tracheal injection of bleomycin (BLM). Second, the clinical manifestations and histopathological changes of the mice were used to verify that treatment with CEP might significantly reduce BLM-induced fibrosis. Furthermore, flow cytometric analysis was used to analyze the changes in the number of M2 macrophages in the lung tissues before and after treatment with CEP to explore the relationship between macrophage M2 polarization and pulmonary fibrosis. In vitro, we constructed two co-culture systems (THP-1 and MRC5 cells, RAW264.7 and NIH 3T3 cells), and measured the expression of fibrosis-related proteins to explore whether CEP could reduce pulmonary fibrosis by regulating macrophage M2 polarization and fibroblast activation.

Results The results showed that the intranasal treatment of CEP significantly attenuated the symptoms of pulmonary fibrosis induced by BLM in a murine model. Our findings also indicated that CEP treatment markedly reduced the expression of fibrosis markers, including TGF-β1, collagen I, fibronectin and α-SMA, in the mouse lung. Furthermore, in vitro studies demonstrated that CEP attenuated pulmonary fibrosis by inhibiting fibroblast activation through modulating macrophage M2 polarization and reducing TGF-β1 expression.

Conclusions This study demonstrated the potential and efficacy of CEP in the treatment of pulmonary fibrosis. In particular, this study revealed a novel mechanism of CEP in inhibiting fibroblast activation by regulating macrophage

[†]Jiaqi Bao, Chang Liu and Huafeng Song contributed equally to this work.

[†]Shufa Zheng and Yu Chen contributed equally to this work.

*Correspondence:
Shufa Zheng
zsfzheng@zju.edu.cn
Yu Chen
chenyuzy@zju.edu.cn

Full list of author information is available at the end of the article

M2 polarization and reducing the expression of fibrosis-associated factors. Our findings open a new direction for future research into the treatment of pulmonary fibrosis.

Keywords Pulmonary fibrosis, Cepharanthine, Macrophage polarization

Background

Pulmonary fibrosis is the end stage of a broad range of heterogeneous interstitial lung diseases. IPF, the most common form of pulmonary fibrosis, is a chronic, progressive and fatal condition interstitial pneumonia characterized by myofibroblast proliferation and ECM deposition [1–3]. The etiology of IPF is complex, and the median survival of patients is only 2 to 3 years from diagnosis [4, 5]. The treatment options for this condition are limited, as only two drugs, pyrifenidone and nittidanib, are currently approved by the FDA [6, 7]. This provides patients with limited hope for survival.

Although the pathogenesis has not been fully elucidated, IPF has a complex etiology that can result from more than 200 factors, such as chemicals, smoking, viral infections and radiation [8]. In response to these factors, alveolar epithelial cells are damaged and undergo aberrant repair, fibroblasts proliferate and activate, and the ECM is excessively deposited, which together results in fibrotic changes in the lungs [9, 10]. In this context, macrophages, as key immune cells in the lung, play important regulatory roles in the pathogenesis of IPF [11, 12]. During the course of IPF, macrophages are induced to migrate and polarize, resulting in two phenotypes with different functional states: the pro-inflammatory M1 phenotype and the anti-inflammatory M2 phenotype [13, 14]. Current studies suggest that M2 macrophages can trigger pathological fibrotic repair mechanisms and facilitate organ fibrosis [15]. The pro-fibrotic effects of M2 macrophages are related mainly to the recruitment and proliferation of fibroblasts, which induce epithelial-to-mesenchymal transition (EMT) and fibroblast-to-myofibroblast transition (FMT) through the secretion of fibrotic mediators, especially TGF-β1 [16, 17]. In fact, EMT represents a common downstream mechanism in all fibrotic diseases [18], and can exacerbate IPF progression by enhancing cell migration and invasion during fibrosis and promoting ECM remodelling [19]. A recent study has shown that nuclear factor I-B (NFIB) attenuates IPF by reducing EMT and alveolar structural disruption, whereas miR-326 has the potential to reverse pulmonary fibrosis by mediating NFIB overexpression to block TGF-β-induced EMT [20]. It is worth mentioning that myofibroblasts are widely regarded as the core effector cells responsible for fibrosis, and myofibroblast activation and proliferation are precisely regulated by M2 macrophages and TGF-β1 during the pathology of IPF. Additionally, TGF-β1 produced by macrophage infiltration and the proliferation of activated fibroblasts enhances α-SMA and collagen synthesis and promotes EMT and FMT through the Smad signaling pathway, ultimately driving the development of pulmonary fibrosis [21, 22]. Thus, precise inhibition strategies targeting M2 macrophage polarization and fibroblast activation may lead to more effective treatment options for IPF patients [23].

CEP is a naturally occurring alkaloid derived from Stephania Cephalantha Hayata with various biological functions [24]. It is the only bisbenzylisoquinoline alkaloid approved for human use and has been used in the clinic for more than 70 years, which is often used for the treatment of chronic inflammatory diseases, viral infections, cancer, and immune disorders [25, 26]. Many studies have shown that CEP has excellent anti-SARS-CoV-2 properties, and it has good potential for treating pulmonary fibrosis caused by COVID-19 [27, 28]. However, the mechanism and specific pathways by which CEP attenuates pulmonary fibrosis need to be explored. To this end, we used a murine model of BLM-induced pulmonary fibrosis in the present study, aiming to reveal the role of CEP in mediating macrophages and the potential mechanisms involved in the treatment of pulmonary fibrosis. We found that CEP administration significantly ameliorated BLM-induced pulmonary dysfunction in mice. Therefore, it is reasonable to believe that the potential of CEP as a novel anti-pulmonary fibrosis agent should not be underestimated. Furthermore, CEP may inhibit the activation of fibroblasts through reducing the M2 polarization of macrophages, opening a new path for the treatment of pulmonary fibrosis. This is the first study to reveal the role and mechanism of CEP in attenuating pulmonary fibrosis by modulating macrophage M2 polarization. Our findings not only provide a scientific basis for the potential efficacy of CEP but also highlight directions for the development of future anti-pulmonary fibrosis agents.

Materials and methods

Chemicals

CEP and BLM were purchased from Solarbio (Beijing, China). IL-4 and IL-13 were purchased from PeproTech (Rocky Hill, New Jersey, USA). The sodium chloride injection was obtained from Harbin Sanlian Pharmaceutical (Harbin, China).

Mice

Six- to eight-week-old male C57BL/6 mice were used in this study. Mice were housed in a special pathogen-free, temperature- and humidity-controlled (23 °C±2 °C and

50% relative humidity) room with a 12-h light/dark cycle. Water and rodent chow were provided *ad libitum*. All mouse experiments were approved by the Animal Experimentation Ethics Committee of the First Affiliated Hospital College of Medicine, Zhejiang University.

Establishment of the pulmonary fibrosis murine model in vivo

All of the mice were acclimated for 7 days. The pulmonary fibrosis murine model was generated via tracheal injection as previously reported with minor modifications [29], and the day of surgery was considered day 0. After intraperitoneal anaesthesia with 1% pentobarbital sodium, the mice were randomized into four groups: (1) the saline group: each mouse was intratracheally injected with 25 μL of 0.9% saline on day 0 and then given 25 μL of saline nasal drops from day 1 for 7 consecutive days; (2) the CEP group: each mouse was intratracheally injected with saline as in the saline group and was given CEP (10 mg/kg) in a 25 μL nasal drop from day 1 to day 7; (3) the BLM group: each mouse was intratracheally administered 2 mg/kg BLM (25 μL) on day 0 and then given 25 μL of 0.9% saline nasal drops for 7 consecutive days; (4) the BLM+CEP group: the mice were intratracheally injected with BLM as in the BLM group and were given CEP (10 mg/kg) in a 25 μL volume from day 1 to day 7. During the experiment, the body weights of the mice were recorded daily, and survival rates were measured. Prior to the euthanasia of mice by decapitation, the animals are anaesthetised with a dose of 1% pentobarbital sodium at a dose of 40 mg/kg. This is based on both the existing literature and previous experience gained in our laboratory. This method is regarded as an effective euthanasia method due to its rapid induction of unconsciousness and the alleviation of distress experienced by the mice at the time of death. The sera were then collected and stored at -80 °C until use. The lungs were either instantly frozen in liquid nitrogen and kept at -80 °C or fixed in 4% paraformaldehyde for further analysis. After the lungs were removed, the lung coefficient was also calculated according to the formula "lung coefficient=lung wet mass/body mass × 100%".

Cell treatment

The RAW 264.7, THP-1, NIH 3T3 and MRC5 cell lines were purchased from the Cell Bank of Typical Culture Preservation Commission, Chinese Academy of Sciences. MRC5, NIH 3T3 and RAW 264.7 cells were cultured in Dulbecco's Modified Eagle Medium (DMEM; Gibco, USA), and THP-1 cells were maintained in RPMI 1640 medium (Gibco, USA) supplemented with 10% fetal bovine serum (FBS; Gibco, USA), penicillin (100 U/mL) and streptomycin (100 mg/mL) (Gibco, USA). The cells were maintained in a 5% CO_2 incubator at 37 °C.

Cell counting Kit-8 (CCK8) assay

Cell viability was analyzed by a CCK8 assay (Dojindo Laboratories, Japan) according to the manufacturer's protocols. The cells were seeded and cultured in a 96-well microplate at a density of 5×10^3/well in 100 μL of medium (Corning, USA). Then, the cells were treated with various concentrations of CEP (0, 0.125, 0.250, 0.500, 1 and 2 μg/mL). After treatment for 24 h, 10 μL of CCK8 reagent was added to each well, and the samples were then cultured for 2 h. All the experiments were performed in triplicate. The absorbance was analyzed at 450 nm via the SpectraMax i3x detection system (Molecular Devices, USA).

Histological and immunohistochemical (IHC) analysis

The mice were sacrificed, and the lungs were harvested on day 21 and 28 after the initial treatment. For histological analysis, the lungs were fixed with 10% neutral formalin, embedded in paraffin, and then sectioned transversely (4 μm thick). The sections were then stained with hematoxylin and eosin (H&E). The deposition of collagen fibres in the lungs was measured via Masson's trichrome staining via conventional protocols. For IHC staining, the embedded sections were dewaxed, and antigens were retrieved via sodium citrate heating. Endogenous peroxidase was removed by adding 0.3% H_2O_2 in methanol. Then, the sections were blocked for 90 min with 3% BSA (Sigma-Aldrich, USA) in PBS and incubated with primary antibodies (Supplementary Table 1) at 4 °C overnight. The next day, the sections were rinsed and incubated with secondary antibodies (Supplementary Table 1) for 90 min at room temperature. IHC staining was performed using a 3,3′-diaminobenzidine (DAB) substrate kit (Abcam, USA), and the samples were counterstained with hematoxylin. The images were reviewed and photographed using an Olympus BX 53upright microscope (Olympus, Japan).

Hydroxyproline (HYP) assay

The collagen content in the lung homogenates was evaluated via an HYP Content Assay Kit (Solarbio, Beijing, China). The lung tissues of the mice were homogenized with 1 mL of a 6 mol/L hydrochloric acid solution and hydrolysed at 95 °C for 5 h, and the pH was adjusted to 6.0–8.0. The corresponding reagents were added to the reaction system and incubated at 60 °C for 15 min. After cooling, the supernatants were collected via centrifugation at 6000 rpm for 10 min. The absorbance of each sample was read at 560 nm using the SpectraMax i3x detection system (Molecular Devices, USA).

qRT-PCR analysis of Gene expression

Total RNA was isolated from cells and lung tissues via TRIzol reagent (Thermo Fisher Scientific). Reverse

transcription reactions were performed using QuantiTect Rev. Transcription Kit (QIAGEN, Germany). Quantitative real-time PCR was performed via a QuantiFast SYBR Green PCR Kit (QIAGEN, Germany) with an ABI 7500 instrument (Applied Biosystems, CA, United States). The forward and reverse primer sequences for specific genes are listed in Supplementary Table 2. Each sample was tested in triplicate. The results of the mRNA quantification were normalized against GAPDH and calculated using the ΔΔ cycle threshold (Ct) method.

Western blotting

The samples were lysed in RIPA lysis buffer on ice. Equal amounts of protein from each sample were separated on SDS-PAGE gels and then transferred to polyvinylidene fluoride (PVDF) membranes (Millipore, USA). The blots were blocked in a 5% nonfat milk/TBST solution at room temperature for 1 h and incubated with primary antibodies (Supplementary Table 1) at 4 °C overnight. The membranes were washed with TBS containing 0.1% Tween 20 to remove unbound primary antibodies and incubated with fluorescent secondary antibodies (Supplementary Table 1) at room temperature for 1 h. After another wash with TBS containing 0.1% Tween 20, the protein bands were visualized with a Bio-Rad ChemiDoc MP multifunction chemiluminescence imager (Bio-Rad, USA) and analyzed via Image Lab™ software.

Flow cytometry

Fresh mouse lung tissues were cut into approximately $1mm^3$ pieces and enzymatically digested with collagenase IV (Solarbio, Beijing, China) for 30 min at 37 °C. The dissociated cells were subsequently passed through a 70-μm cell strainer and centrifuged at 400 × g for 10 min. The pelleted cells were then resuspended and incubated with red blood cell lysis buffer (Solarbio, China) on ice for 5 min to lyse the red blood cells. After being washed twice with PBS, the cells were resuspended in stain buffer (BD Pharmingen, USA) and kept on ice. First, the cells were stained for viability assays using Fixable Viability Stain 700 (BD Pharmingen, USA). 100 μL of the cell suspension was removed and stained with the following surface antibodies: BV750 rat anti-mouse F4/80 (BD Pharmingen, USA), APC-Cy7 rat anti-mouse CD45 (BD Pharmingen, USA), BV480 rat anti-CD11b (BD Pharmingen, USA), anti-CD163TNKUPJPE-CYN7 (Thermo, USA), and BV605 rat anti-mouse CD86 (BD Pharmingen, USA). After fixation rupture using the Fixation/Permeabilization Kit (BD Pharmingen, USA), the cells were stained with the following intracellular antibodies: FITC mouse anti-iNOS/NOS Type II (BD Pharmingen, USA) and Alexa Fluor 647 rat anti-mouse CD206 (BD Pharmingen, USA). The cells were maintained at 4 °C and analyzed on a BECKMAN CytoFLEX (Cytek Biosciences, USA). The data were analyzed via FlowJo (v.10.6.2).

Immunofluorescence (IF) staining

The cells and sections were fixed with 4% paraformaldehyde (Thermo Fisher Scientific, USA), permeabilized with 0.1% Triton X-100 (Sigma-Aldrich, USA), and then blocked with 3% BSA (Sigma-Aldrich, USA). The cells and sections were subsequently incubated with specific primary antibodies overnight at 4 °C. Collagen I, fibronectin and α-SMA primary antibodies were used, and detailed information can be found in Supplementary Table 1. On the subsequent day, the cells and sections were stained with Alexa Fluor 488-labelled secondary antibodies (Supplementary Table 1) in the dark for 1.5 h at room temperature. Nuclear staining was performed with DAPI (YEASEN Biotech Co., Ltd., China; 0.5 μg/mL in PBS) for 10 min at room temperature. The images were observed using an Olympus FV3000 confocal laser scanning microscope imaging system (Olympus, Japan).

Enzyme-linked immunosorbent assay (ELISA)

The concentrations of IL-6, TNF-α, TGF-β1, and IL-1β in the serum or culture supernatants were analyzed via ELISA kits (Proteintech, USA) according to the manufacturer's instructions. The absorbance was measured at 450 nm with the correction wavelength set at 630 nm using the SpectraMax i3x detection system (Molecular Devices, USA).

Statistical analysis

Statistical analysis was conducted via GraphPad Prism 9.0 (San Diego, USA). The data were expressed as the means ± standard deviations (SDs). Differences in the body weight gain ratios of the mice were analytically assessed via repeated measures analysis of variance (ANOVA). P values between two groups were analyzed via Student's t test. When the data were included in three or more groups, P values were calculated via one-way ANOVA. $P<0.05$ was considered statistically significant.

Results

CEP ameliorates BLM-induced pulmonary fibrosis in mice

In the present study, the protective function of CEP against BLM-induced pulmonary fibrosis was revealed by comparing the results of body weight changes, survival rates, pulmonary pathological manifestations, lung coefficients, and HYP measurements between the CEP group and the BLM + CEP group of mice. A murine model was established by tracheal injection of BLM and intranasal treatment with CEP to explore the effects of CEP on pulmonary fibrosis (Fig. 1A). The mice were injected intratracheally with BLM (2.0 mg/kg) or saline on day 0. The saline group and BLM group were then treated with

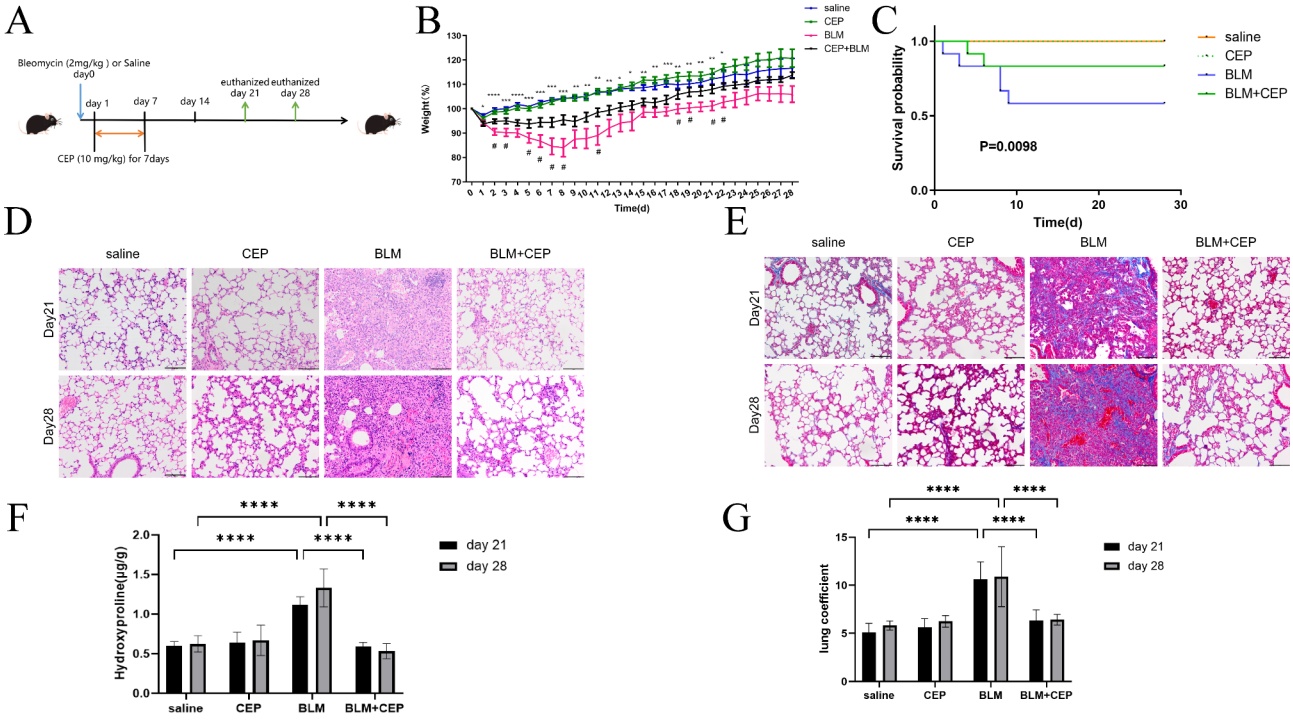

Fig. 1 CEP exerts an anti-fibrotic effect on BLM-induced pulmonary fibrosis in mice. **(A)** Schematic representation of the experimental design. **(B)** Mean changes in body weight in each group ($n=11$). Body weight was expressed as a percentage of day 0 body weight. *$P<0.05$, **$P<0.01$, ***$P<0.001$ and ****$P<0.0001$ (BLM group vs. saline group); #$P<0.05$ (BLM group vs. BLM+CEP group). **(C)** Kaplan–Meier survival curves of different groups of mice ($n=12$). **(D)** Pathological structure changes in the lung tissue of the mice at day 21 and day 28, as determined by H&E staining (original magnification, ×200, scale bar = 100 μm, $n=3$). **(E)** Changes in the lung tissue of the mice at day 21 and day 28, as determined by Masson's trichrome staining (original magnification, ×200, scale bar = 100 μm, $n=3$). **(F)** HYP content in the lung tissues of the mice in each group ($n=6$). **(G)** Lung coefficients for each group of mice at day 21 and day 28. ****$P<0.0001$

saline via the nasal route for 7 days, while the CEP group and the BLM+CEP group were treated with CEP via the nasal route. The mice were euthanized, and samples were collected for analysis on day 21 and day 28 after BLM instillation. As shown in Fig. 1B, compared with those in the saline group, the body weights were significantly lower after BLM infusion ($P<0.05$), whereas there was no significant difference in body weight, animal survival rate or pathological structure changes in the CEP group, indicating the safe use of CEP in vivo (Fig. 1B-E). In contrast, the body weights of the mice in the BLM+CEP group were significantly higher than those of the mice in the BLM group ($P<0.05$, Fig. 1B). BLM exposure led to poorer survival rates than saline exposure did, but CEP treatment reduced the mortality of BLM-challenged mice ($P<0.05$, Fig. 1C). As shown in Fig. 1D and E, histological changes on day 21 and day 28 revealed no inflammation or fibrosis in the lung tissue of the saline or CEP groups. However, the BLM group exhibited disturbed alveolar structure, thickened airway walls and collagen deposition. After CEP treatment, the alveolar structure was restored, the alveolar wall thickness decreased, and collagen deposition was reduced. To quantify the extent of pulmonary fibrosis, we measured the HYP content in the lung tissue of each group. As a core component of collagen, HYP is a key indicator of collagen metabolism and degree of fibrosis. As shown in Fig. 1F, compared with saline injection, BLM injection significantly increased the HYP content in the lung tissue at day 21 and day 28 ($P<0.0001$), whereas the HYP content in the lung tissue was significantly lower in the BLM+CEP group than that in the BLM group ($P<0.0001$). In addition, on day 21 and day 28, the mean lung coefficients of the CEP and saline groups were similar, whereas the BLM group presented significantly greater lung coefficients than did the saline group ($P<0.0001$, Fig. 1G). We also found that the lung coefficient of the BLM+CEP group was smaller than that of the BLM group ($P<0.0001$). These findings initially revealed the protective effects of CEP on BLM-induced pulmonary fibrosis.

CEP treatment reduces fibroblast activation and ECM deposition in mouse lungs

The activation of fibroblasts and excessive deposition of ECM play key roles in the onset and progression of pulmonary fibrosis [30]. To further reveal that CEP inhibits BLM-induced ECM deposition in mice to ameliorate lung fibrosis, the levels of components of the ECM [31], such

as α-SMA, fibronectin, and collagen I, were measured. IHC staining revealed that the levels of α-SMA, fibronectin and collagen I were strongly elevated on day 21 and day 28 after BLM challenge but strongly ameliorated in CEP-treated mice compared with those in BLM-treated mice (Fig. 2A-C). IF staining revealed that after BLM injection, the α-SMA protein level was elevated on day 21 and day 28 (Fig. 2D-E). The mRNA levels of fibrotic genes were markedly greater in the BLM group than those in the saline group on day 21 and day 28 ($P<0.05$); the changes in the mRNA levels were dramatically reversed after CEP treatment (Fig. 2F-H). As shown in Fig. 2I-J, the protein levels of fibronectin, collagen I and α-SMA in the lungs were strongly lower in the BLM+CEP group

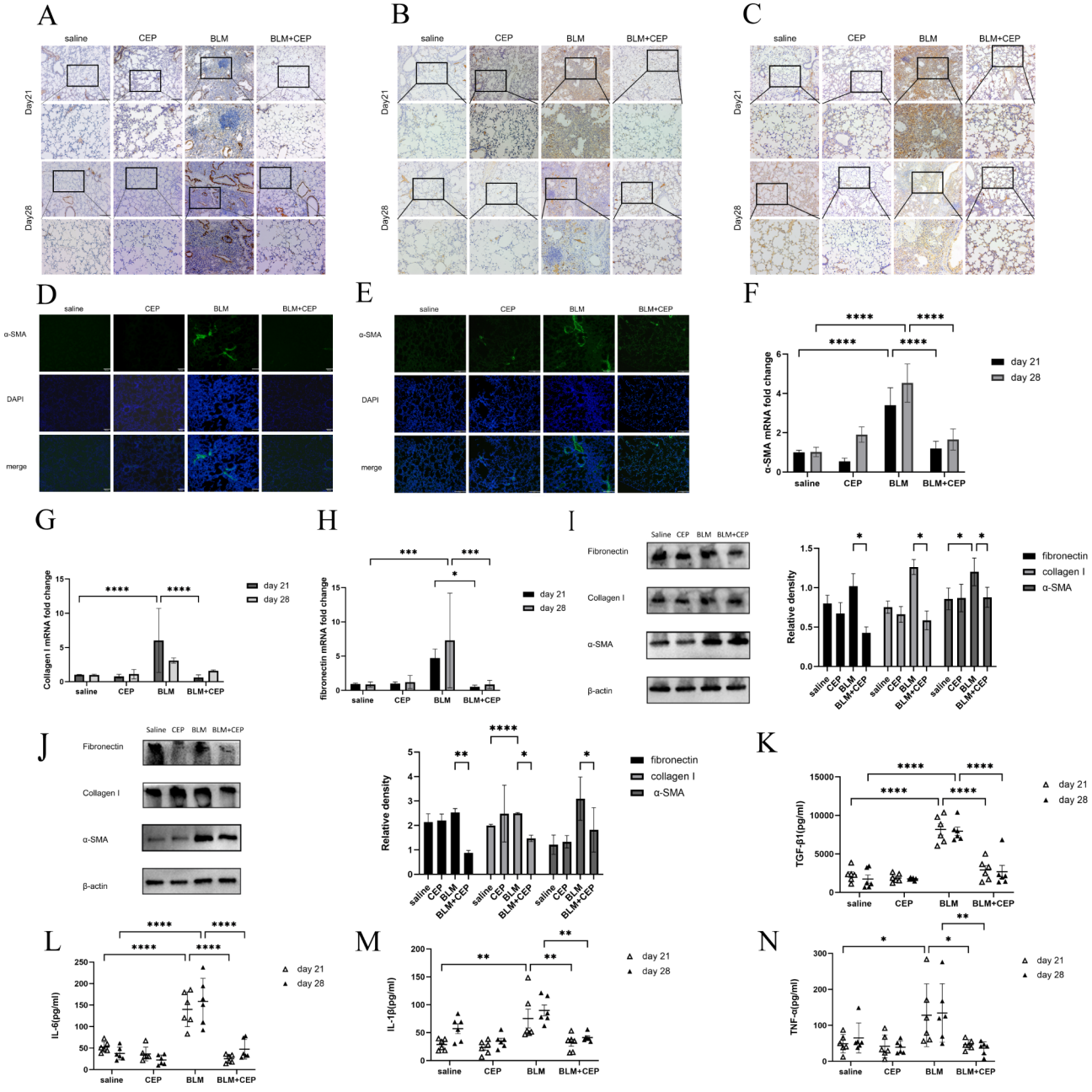

Fig. 2 CEP reduces BLM-induced fibroblast activation and collagen deposition in mice. **(A-C)** IHC staining of α-SMA **(A)**, collagen I **(B)** and fibronectin **(C)** in the lung tissues of the mice in each group on day 21 and 28 (original magnification, ×100; scale bar = 200 μm; $n=3$). **(D-E)** IF staining of α-SMA in mouse lungs on day 21 **(D)** and day 28 **(E)** (original magnification, ×100; scale bar = 200 μm; $n=3$). **(F-H)** Changes in the mRNA levels of α-SMA **(F)**, collagen I **(G)** and fibronectin **(H)** in mouse lungs ($n=6$). **(I-J)** Protein levels of fibronectin, collagen I and α-SMA in mouse lungs on day 21 (**I**, $n=3$) and day 28 (**J**, $n=3$). The density of the bands from per group was analyzed via Image-J software and normalized to the number of arbitrary units of β-actin. (K-N) Serum levels of TGF-β1 **(K)**, IL-6 **(L)**, IL-1β **(M)**, and TNF-α **(N)** in the mice ($n=6$). *$P<0.05$, **$P<0.01$, ***$P<0.001$ and ****$P<0.0001$

than those in the BLM group ($P<0.05$). These results suggest that CEP can attenuate the progression of pulmonary fibrosis in vivo by reducing ECM deposition. TGF-β1 is currently recognized as the most potent fibrogenic cytokine [32], promoting fibroblast proliferation. Additionally, IL-1β, IL-6 and TNF-α also promote fibroblast activation, and are involved in ECM synthesis [33]. The levels of serum TGF-β1, IL-6, IL-1β, and TNF-α were significantly increased after BLM injection compared with those in the saline group and were decreased after CEP treatment (Fig. 2K-N). Therefore, CEP improves pulmonary fibrosis by reducing fibroblast activation and decreasing ECM deposition.

CEP inhibits M2 polarization of macrophages in BLM-induced pulmonary fibrosis

The number of macrophages, important immune sentinels that promote homeostasis in the lungs, increases significantly upon stimulation, thereby causing inflammation and fibrosis [34, 35]. Moreover, polarized M1/M2 macrophage populations are strongly associated with the development of inflammation and the production of fibrotic mediators in pulmonary fibrosis [36]. To explore the effect of CEP on the polarization of macrophages, the number of M2 macrophages in each group of fibrotic mice on day 21 and day 28 was analyzed via flow cytometry. After the exclusion of adhesions, dead cells may also be excluded via live/dead staining, and macrophages can be readily identified on the basis of F4/80 and CD11b expression [37] (Supplementary Fig. 1). Given that CD206 is positively expressed in M2 subpopulations, which are mainly responsible for the induction of tissue fibrosis, $CD11b^+$ $F4/80^+$ $CD206^+$ M2 macrophages were then analyzed (Fig. 3A). As shown in Fig. 3B and C, the percentage of $CD206^+$ M2 macrophages was significantly greater in the BLM-induced group than in the saline group on day 21 and was significantly lower after CEP treatment ($P<0.0001$). Consistent results were observed on day 28 (Fig. 3D and E). However, CEP treatment did not significantly affect the number of $iNOS^+$ M1 macrophages(Supplementary Fig. 2). These results suggest that CEP can reduce the number of M2 macrophages. The amelioration of BLM-induced pulmonary fibrosis by CEP treatment may be associated with a reduction in the M2 polarization of macrophages.

The blocking effect of CEP on fibroblast activation is achieved mainly through the regulation of M2 polarization of macrophages

The transformation of fibroblasts is the main source of activated myofibroblasts in pulmonary fibrosis [38], and macrophage polarization may play an important role in this process. M2 macrophages induced by IL-4 or IL-13 promote the secretion of the pro-fibrotic factor TGF-β1 [39]. To explore whether the blocking effect of CEP on fibroblast activation is achieved mainly by regulating the M2 polarization of macrophages, we established two co-culture systems, as shown in Fig. 4B: (1) IL-4-dependent RAW264.7 cells co-cultured with NIH 3T3 cells and (2) IL-4- and IL-13-dependent THP-1 cells co-cultured with MRC5 cells. First, after treatment with various concentrations of CEP for 24 h and 48 h, CCK-8 assays were

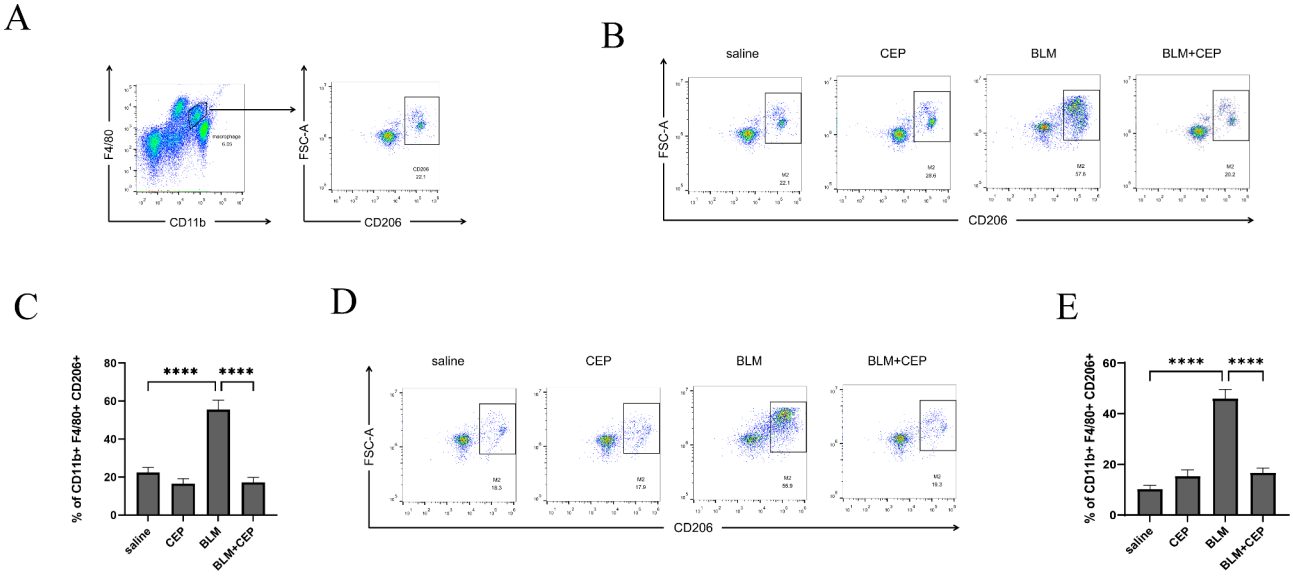

Fig. 3 CEP decreases the number of M2 macrophages in BLM-induced mice. **(A)** $F4/80^+$ $CD11b^+$ macrophages isolated from digested mouse lungs were gated, and M2 macrophages ($CD11b^+$ $F4/80^+$ $CD206^+$) were then analyzed by flow cytometry. **(B)** Percentages of $CD11b^+$ $F4/80^+$ $CD206^+$ cells in the saline, CEP, BLM and BLM + CEP groups on day 21 ($n=6$). **(C)** Statistical results of **(B)**. **(D)** Percentages of $CD11b^+$ $F4/80^+$ $CD206^+$ cells in the saline, CEP, BLM and BLM + CEP groups on day 28 ($n=6$). **(E)** Statistical results of **(D)**. ****$P<0.0001$

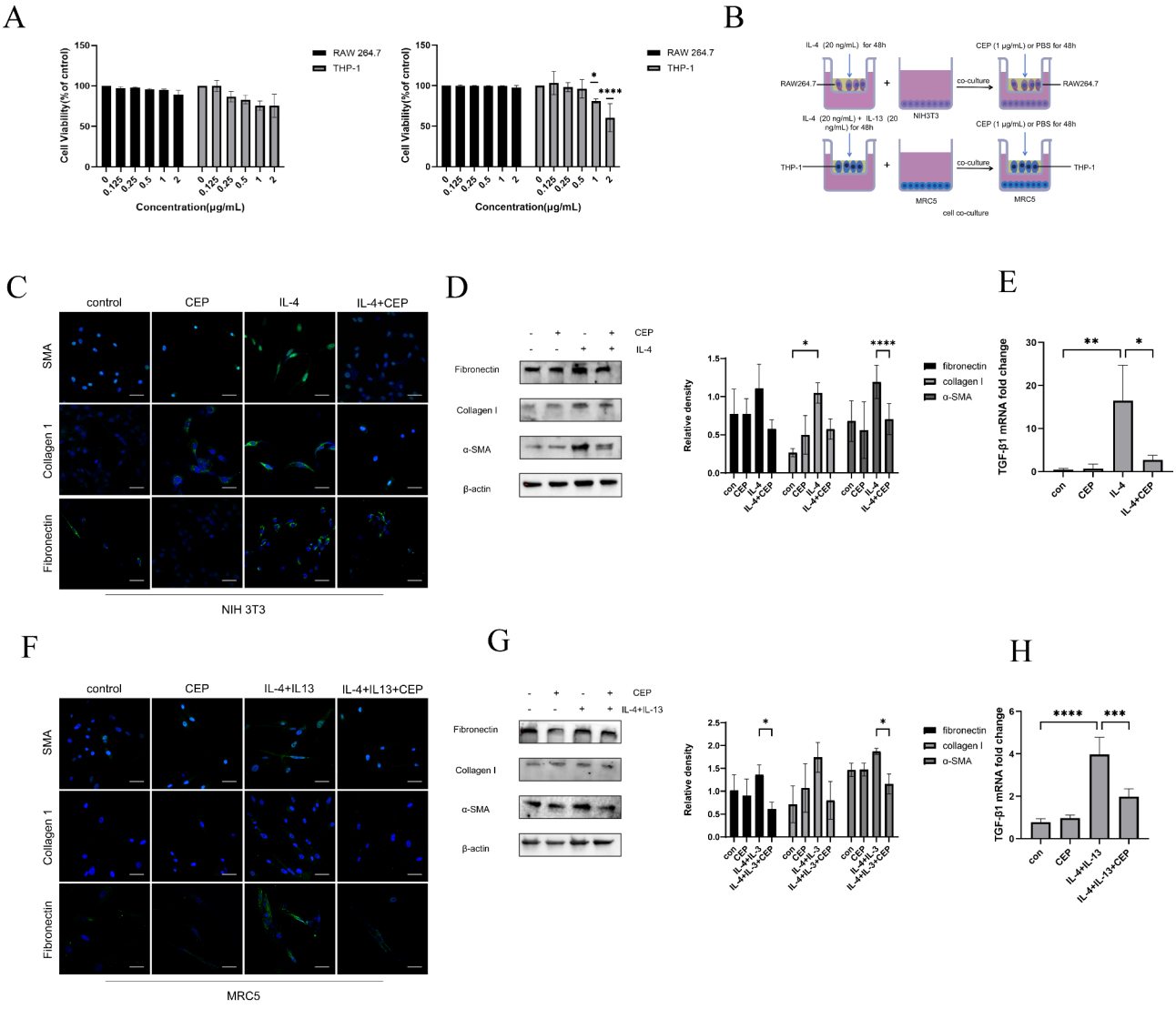

Fig. 4 CEP inhibits the M2 polarization of macrophages. **(A)** CCK-8 assay of RAW264.7 and THP-1 cells after CEP treatment at 0, 0.125, 0.250, 0.500, 1 and 2 μg/mL for 24 h (left panel) and 48 h (right panel). The data are presented as the means ± SDs of three independent experiments. **(B)** RAW264.7 cells were cultured alone or with IL-4 (20 ng/mL) for 48 h to induce M2 polarization in macrophages. Next, the cell culture inserts containing the pre-treated macrophages were transferred to plates seeded with NIH 3T3 cells. RAW264.7 cells were treated with 0.500 μg/mL CEP as indicated. THP-1 cells were cultured alone or with IL-4 (20 ng/mL) and IL-13 (20 ng/mL) for 48 h to induce M2 polarization of the macrophages. THP-1 cells were treated with 0.500 μg/mL CEP, and a co-culture system was established. **(C)** IF staining of fibronectin, collagen I and α-SMA in NIH 3T3 cells (green). The cell nuclei were counterstained with DAPI (blue). (original magnification, ×400; scale bar = 50 μm; $n = 3$) **(D)** Protein levels of fibrotic markers, including fibronectin, collagen I and α-SMA, in NIH 3T3 cells were measured via western blotting ($n = 3$). The density of the bands from each group was analyzed via Image-J software and normalized by the number of arbitrary units of β-actin. **(E)** The relative expression of TGF-β1 mRNA in RAW264.7 cells. **(F)** IF staining of fibronectin, collagen I and α-SMA in MRC5 cells (green). The cell nuclei were counterstained with DAPI (blue). (original magnification, ×400; scale bar = 50 μm; $n = 3$) **(G)** The protein levels of fibronectin, collagen I and α-SMA in MRC5 cells were measured by western blotting ($n = 3$). The density of the bands from each group was analyzed via Image-J software and normalized by the number of arbitrary units of β-actin. **(H)** The relative expression of TGF-β1 mRNA in THP-1 cells. $^{*}P < 0.05$, $^{**}P < 0.01$, $^{***}P < 0.001$ and $^{****}P < 0.0001$

performed to analyze the effect of CEP on the viability of macrophages. For THP-1 cells, treatment with CEP at concentrations of 1 μg/mL and 2 μg/mL had a strong effect on the cell survival rate after 48 h. However, CEP did not inhibit the growth of RAW264.7 cells at all concentrations (Fig. 4A). In this study, 0.500 μg/mL CEP was used. As shown in Fig. 4B, RAW264.7 cells were co-cultured with NIH 3T3 cells pre-treated with IL-4. Compared with macrophages that were not polarized, macrophages co-cultured with NIH 3T3 cells after induced polarization presented increased fluorescence intensity for NIH 3T3 fibronectin, collagen I and α-SMA, whereas the fluorescence intensity of these proteins was significantly reduced after CEP treatment

(Fig. 4C). Western blotting revealed increased expression of collagen I, α-SMA and fibronectin in NIH 3T3 cells co-cultured with IL-4-pretreated RAW246.7 cells and decreased expression after treatment with CEP (Fig. 4D). As shown in Fig. 4E, TGF-β1 was elevated after macrophage polarization and decreased after treatment with CEP ($P<0.05$). A similar phenomenon was observed for MRC5 cells in the co-culture system (Fig. 4B). The fluorescence intensity of fibronectin, collagen I and α-SMA increased when MRC5 cells were co-cultured with THP-1 cells pre-treated with IL-4 and IL-13, and the fluorescence intensity of these proteins was significantly reduced after CEP treatment (Fig. 4F). As shown in Fig. 4G, the western blotting results were consistent with those of the NIH 3T3 co-culture system. The expression of TGF-β1 in THP-1 cells was elevated after M2 polarization and decreased after CEP treatment ($P<0.001$, Fig. 4H). These results suggest that the blocking effect of CEP on fibroblast activation may be related to the inhibition of M2 polarization of macrophages.

Discussion

The present study revealed the significant protective effect of CEP on pulmonary fibrosis both in vivo and in vitro. Specifically, we demonstrated that CEP significantly reduced BLM-induced inflammation, collagen deposition, lung coefficients, and the levels of several inflammatory factors, including TGF-β1, IL-1β, IL-6, and TNF-α. Furthermore, our research demonstrated that CEP effectively inhibited fibroblast activation by modulating macrophage M2 polarization in vitro, thereby attenuating lung fibrosis. Given that IPF is a complex and intractable disease with intricate pathogenesis, there is still no conclusive and effective treatment for it [10, 40]. Thus, these positive effects demonstrated by CEP not only provide new hope for the treatment of pulmonary fibrosis, but also open a new chapter in the in-depth exploration of its mechanism of action.

Our findings do not stand alone; in fact, they echo and complement the findings of other researchers. Similar to our findings, Li et al. demonstrated that CEP has a certain therapeutic effect on pulmonary fibrosis by attenuating BLM-induced collagen accumulation and inflammation in rats, thus exerting a protective effect on pulmonary fibrosis [28]. Ma et al. also reported that CEP affects the respiratory burst activity of alveolar macrophages, resulting in a broad anti-fibrotic effect in a rat model [41]. In addition, CEP has excellent anti-SARS-CoV-2 properties, and Rogosnitzky et al. reported that it has good potential for treating pulmonary fibrosis caused by COVID-19 [24, 27, 28]. Additionally, Huang et al. found that the levels of pro-inflammatory cytokines, including TNF-α, IL-1β and IL-6, were indeed downregulated after CEP treatment and that lung histopathological changes were attenuated in a murine model of LPS-induced lung inflammatory injury, which supported our findings [42].

In fact, macrophages play a key role in the development of IPF because of their plasticity and ability to differentiate into different macrophage subpopulations [12–14]. Tissue-resident macrophages (M0) are multifunctional cells that exhibit a high degree of plasticity and are more typically represented by classically activated M1 or alternatively activated M2 macrophages [43]. Analysis of macrophage polarization in the lung tissue via flow cytometry revealed a more pronounced increase in the percentage of M2 macrophages but not M1 macrophages in the BLM group, whereas the percentage of M2 macrophages was reduced in the BLM+CEP group. The reduction in M2 macrophages after CEP treatment suggests that CEP may regulate fibrosis progression by modulating M2 polarization. M2 macrophages had anti-inflammatory effects, promote angiogenesis and tissue remodeling and may be associated with fibrotic diseases, including pulmonary fibrosis [44]. Moreover, Redente et al. reported high numbers of M2 macrophages in heavily fibrotic lung tissue [44, 45]. Rui et al. reported that reducing M2 macrophage polarization improved pulmonary fibrosis during pulmonary fibrosis therapy via eucalyptol, which could explain our findings [46]. Pushpakom et al. found that CEP could alleviate kidney tubular dysfunction by regulating macrophages [47]. In addition, M2 macrophages can produce cytokines such as TGF-β1 to promote fibrosis [48], and the reduction in these factors that we found in the BLM+CEP group may have been achieved by reducing the number of macrophages in the M2 population.

There is increasing evidence that IPF is associated with fibroblast activation and macrophage polarization and that there is a link between these two cell types [49]. During the process of fibrosis, fibroblasts act as key effector cells through over-activation and aberrant differentiation via the EMT pathway [21, 22], whereas M2 macrophage differentiation and increased pro-fibrotic factors create a microenvironment that sustains fibrogenesis. In this study, we focused on M2 macrophage polarization and demonstrated that CEP could inhibit M2 polarization of macrophages and fibroblast activation in lung tissues in vivo. Furthermore, our results provide evidence for the pro-fibrotic role of IL-4- and IL-13-induced M2 macrophages in fibroblast activation and IPF development. This finding is consistent with the findings of Wang et al., who reported that microcystin-LR modulated M2 macrophage polarization and inhibited EMT and FMT in fibroblasts when MRC5 or NIH 3T3 cells were co-cultured with RAW264.7 cells pre-treated with IL-4 to induce polarization [50]. A number of studies have also demonstrated that therapies that target M2 macrophages and inhibit fibroblast activation may potentially

attenuate lung fibrosis [35]. Sakaguchi et al., on the other hand, found that CEP prevents lethality or cytotoxicity by inhibiting endotoxin-induced NO in macrophages and that its action may be mediated by enhancing fibroblast proliferation [49]. Overall, CEP is therapeutically relevant in the development of IPF via modulating M2 macrophage polarization.

Strengths and limitations

The present study demonstrates significant strengths in exploring the role and potential mechanisms of CEP in the treatment of pulmonary fibrosis. To begin with, we demonstrated the remarkable capacity of CEP to mitigate pulmonary dysfunction in mice through the utilization of a murine model of BLM-induced pulmonary fibrosis. This provides a theoretical and experimental foundation for the prospective clinical application of CEP. Moreover, a deeper exploration of the mechanism of CEP in alleviating pulmonary fibrosis was carried out in this study, which revealed for the first time that CEP may inhibit fibroblast activation by suppressing the M2 polarization of macrophages, which ultimately ameliorates pulmonary fibrosis. These vital findings not only reveal a new mechanism of CEP in the treatment of pulmonary fibrosis but also have promising theoretical value.

We acknowledge several limitations in the present study. First, we explored the application of CEP in pulmonary fibrosis, but it is limited to animal and cellular models. The clinical application of CEP needs to be further verified. Second, the specific mechanism of CEP in the treatment of pulmonary fibrosis has not been fully elucidated. Further analysis of the molecular mechanisms and signalling pathways by which CEP regulates pulmonary fibrosis is needed.

Conclusions

In conclusion, we established a link between lung macrophage polarization and pulmonary fibrosis in a murine model and revealed the therapeutic potential of CEP for this disease. Our findings demonstrated that CEP attenuated lung inflammation and ameliorated pathological changes in the lung tissue of mice with BLM-induced pulmonary fibrosis. The effects of CEP on pulmonary fibrosis may be related to the suppression of macrophage M2 polarization, which reduces fibroblast activation and ECM production. This study offers a useful reference for the treatment of pulmonary fibrosis with traditional Chinese medicine, opening new directions and concepts for the clinical application of CEP. Moreover, further mechanisms remain to be investigated in the future.

Supplementary Information

The online version contains supplementary material available at https://doi.org/10.1186/s12890-024-03250-z.

Supplementary Material 1

Acknowledgements

We acknowledge the contributions of other clinical and laboratory staff at the First Affiliated Hospital, Zhejiang University School of Medicine.

Author contributions

JB and CL were mainly responsible for animal and cell experimental manipulation, data analysis and article writing. HS was responsible for the data research, experimental manipulation and writing of the first draft. ZM, JJ and QW participated in the animal experiments. WQ, FY, and YS analyzed and organized the experimental data. XC designed the overall idea of the project. RW and WC participated in the cellular experiments. SZ was responsible for the design of the project and data analysis. YC was responsible for the design of the project and the revision of the article. All the authors read and approved the final manuscript.

Funding

This work was supported by the National Natural Science Foundation of China (Grant Numbers 81971919, 82072377 and 82300005) and the Young Health Talents Program of Suzhou (Qngg2021028).

Data availability

The datasets used and/or analyzed during the current study are available from the corresponding author upon reasonable request.

Declarations

Ethics approval and consent to participate

The study was reviewed and approved by the Animal Experimentation Ethics Committee of the First Affiliated Hospital College of Medicine, Zhejiang University, with approval number 2023 – 1437. All methods involving animals were carried out in accordance with the ARRIVE (Animal Research: Reporting of In Vivo Experiments) guidelines.

Consent for publication

Not applicable.

Competing interests

The authors declare that they have no known competing financial interests or personal relationships that could have appeared to influence the work reported in this paper.

Author details

[1]Department of Laboratory Medicine, the First Affiliated Hospital, Zhejiang University School of Medicine, 79 Qingchun Road, Hangzhou 310003, China
[2]Key Laboratory of Clinical In Vitro Diagnostic Techniques of Zhejiang Province, Hangzhou 310003, China
[3]Institute of Laboratory Medicine, Zhejiang University, Hangzhou 310003, China
[4]Department of Clinical Laboratory, The Fifth People's Hospital of Suzhou, Infectious Disease Hospital Affiliated to Soochow University, No. 10, Guangqian Road, Xiangcheng District, Suzhou 215000, China

Received: 1 March 2024 / Accepted: 29 August 2024
Published online: 11 September 2024

References

1. Hewlett JC, Kropski JA, Blackwell TS. Idiopathic pulmonary fibrosis: epithelial-mesenchymal interactions and emerging therapeutic targets. Matrix Biol. 2018;71(2):112–27.
2. Lederer DJ, Martinez FJ. Idiopathic pulmonary fibrosis. N Engl J Med. 2018;378(19):1811–23.
3. Wang J, Lai X, Yao S, Chen H, Cai J, Luo Y, Wang Y, Qiu Y, Huang Y, Wei X, Wang B, Lu Q, Guan Y, Wang T, Li S, Xiang AP. Nestin promotes pulmonary fibrosis via facilitating recycling of TGF-β receptor I. Eur Respir J. 2022;59(5):2003721.

4. Raghu G, Collard HR, Egan JJ, Martinez FJ, Behr J, Brown KK, Colby TV, Cordier JF, Flaherty KR, Lasky JA, Lynch DA, Ryu JH, Swigris JJ, Wells AU, Ancochea J, Bouros D, Carvalho C, Costabel U, Ebina M, Hansell DM, Johkoh T, Kim DS, King TE Jr, Kondoh Y, Myers J, Müller NL, Nicholson AG, Richeldi L, Selman M, Dudden RF, Griss BS, Protzko SL, Schünemann HJ, ATS/ERS/JRS/ALAT Committee on Idiopathic Pulmonary Fibrosis. An official ATS/ERS/JRS/ALAT statement: idiopathic pulmonary fibrosis: evidence-based guidelines for diagnosis and management. Am J Respir Crit Care Med. 2011;183(6):788–824.
5. Rudd RM, Prescott RJ, Chalmers JC, Johnston ID, Fibrosing Alveolitis Subcommittee of the Research Committee of the British Thoracic Society. British thoracic society study on cryptogenic fibrosing alveolitis: response to treatment and survival. Thorax Thorax. 2007;62(1):62–6.
6. Richeldi L, du Bois RM, Raghu G, Azuma A, Brown KK, Costabel U, Cottin V, Flaherty KR, Hansell DM, Inoue Y, Kim DS, Kolb M, Nicholson AG, Noble PW, Selman M, Taniguchi H, Brun M, Le Maulf F, Girard M, Stowasser S, Schlenker-Herceg R, Disse B, Collard HR, INPULSIS Trial Investigators. Efficacy and safety of nintedanib in idiopathic pulmonary fibrosis. N Engl J Med. 2014;370(22):2071–82.
7. King TE Jr, Bradford WZ, Castro-Bernardini S, Fagan EA, Glaspole I, Glassberg MK, Gorina E, Hopkins PM, Kardatzke D, Lancaster L, Lederer DJ, Nathan SD, Pereira CA, Sahn SA, Sussman R, Swigris JJ, Noble PW. ASCEND Study Group. A phase 3 trial of pirfenidone in patients with idiopathic pulmonary fibrosis. N Engl J Med. 2014;370(22):2083–92.
8. Wilson MS, Wynn TA. Pulmonary fibrosis: pathogenesis, etiology and regulation. Mucosal Immunol. 2009;2(2):103–21.
9. Moss BJ, Ryter SW, Rosas IO. Pathogenic mechanisms underlying idiopathic pulmonary fibrosis. Annu Rev Pathol. 2022;17:515–46.
10. Mei Q, Liu Z, Zuo H, Yang Z, Qu J. Idiopathic pulmonary fibrosis: an update on Pathogenesis. Front Pharmacol. 2022;12:797292.
11. Isshiki T, Vierhout M, Naiel S, et al. Therapeutic strategies targeting profibrotic macrophages in interstitial lung disease. Biochem Pharmacol. 2023;211:115501.
12. Mutsaers SE, Miles T, Prêle CM, Hoyne GF. Emerging role of immune cells as drivers of pulmonary fibrosis. Pharmacol Ther. 2023;252:108562.
13. Duffield JS, Lupher M, Thannickal VJ, Wynn TA. Host responses in tissue repair and fibrosis. Annu Rev Pathol. 2013;8:241–76.
14. Wynn TA, Barron L. Macrophages: master regulators of inflammation and fibrosis. Semin Pulm Dis. 2010;30:245–57.
15. He L, Jhong JH, Chen Q, Huang KY, Strittmatter K, Kreuzer J, DeRan M, Wu X, Lee TY, Slavov N, Haas W, Marneros AG. Global characterization of macrophage polarization mechanisms and identification of M2-type polarization inhibitors. Cell Rep. 2021;37(5):109955.
16. Murray PJ, Wynn TA. Protective and pathogenic functions of macrophage subsets. Nat Rev Immunol. 2011;11(11):723–37.
17. Wei Y, Kim TJ, Peng DH, Duan D, Gibbons DL, Yamauchi M, Jackson JR, Le Saux CJ, Calhoun C, Peters J, Derynck R, Backes BJ, Chapman HA. Fibroblast-specific inhibition of TGF-β1 signaling attenuates lung and tumor fibrosis. J Clin Invest. 2017;127(10):3675–88.
18. Salton F, Ruaro B, Confalonieri P, Confalonieri M. Epithelial-mesenchymal transition: a major pathogenic driver in idiopathic pulmonary fibrosis? Med (Kaunas). 2020;56(11):608.
19. Chilosi M, Caliò A, Rossi A, et al. Epithelial to mesenchymal transition-related proteins ZEB1, β-catenin, and β-tubulin-III in idiopathic pulmonary fibrosis. Mod Pathol. 2017;30(1):26–38.
20. Pattnaik B, Negi V, Chaudhuri R, et al. MiR-326-mediated overexpression of NFIB offsets TGF-β induced epithelial to mesenchymal transition and reverses lung fibrosis. Cell Mol Life Sci. 2023;80(12):357.
21. Li M, Luan F, Zhao Y, Hao H, Zhou Y, Han W, Fu X. Epithelium-specific deletion of TGF-β receptor type II protects mice from bleomycin-induced pulmonary fibrosis. J Clin Invest. 2011;121:277–87.
22. Zhang L, Wang Y, Wu G, Xiong W, Gu W, Wang CY. Macrophages: friend or foe in idiopathic pulmonary fibrosis. Respir Res. 2018;19:170.
23. Burman A, Tanjore H, Blackwell TS. Endoplasmic reticulum stress in pulmonary fibrosis. Matrix Biol. 2018;68–69:355–65.
24. Rogosnitzky M, Okediji P, Koman I. Cepharanthine: a review of the antiviral potential of a japanese-approved alopecia drug in COVID-19. Pharmacol Rep. 2020;72(6):1509–16.
25. Liu K, Hong B, Wang S, Lou F, You Y, Hu R, Shafqat A, Fan H, Tong Y. Pharmacological activity of Cepharanthine. Molecules. 2023;27(13):5019.
26. Shi L, Wang S, Zhang S, Wang J, Chen Y, Li Y, Liu Z, Zhao S, Wei B, Zhang L. Research progress on pharmacological effects and mechanisms of cepharanthine and its derivatives. Naunyn Schmiedebergs Arch Pharmacol. 2023;396(11):2843–60.
27. Zhang S, Huang W, Ren L, Ju X, Gong M, Rao J, Sun L, Li P, Ding Q, Wang J, Zhang QC. Comparison of viral RNA-host protein interactomes across pathogenic RNA viruses informs rapid antiviral drug discovery for SARS-CoV-2. Cell Res. 2022;32(1):9–23.
28. Li J, Chen G, Meng Z, Wu Z, Gan H, Zhu X, Han P, Liu T, Wang F, Gu R, Dou G. Bioavailability enhancement of Cepharanthine via Pulmonary Administration in rats and its therapeutic potential for Pulmonary Fibrosis Associated with COVID-19 infection. Molecules. 2022;27(9):2745.
29. Ma WH, Li M, Ma HF, Li W, Liu L, Yin Y, Zhou XM, Hou G. Protective effects of GHK-Cu in bleomycin-induced pulmonary fibrosis via antioxidative stress and anti-inflammation pathways. Life Sci. 2020;241:117139.
30. Watanabe S, Markov NS, Lu Z, Piseaux Aillon R, Soberanes S, Runyan CE, Ren Z, Grant RA, Maciel M, Abdala-Valencia H, Politanska Y, Nam K, Sichizya L, Kihshen HG, Joshi N, McQuattie-Pimentel AC, Gruner KA, Jain M, Sznajder JI, Morimoto RI, Reyfman PA, Gottardi CJ, Budinger GRS, Misharin AV. Resetting proteostasis with ISRIB promotes epithelial differentiation to attenuate pulmonary fibrosis. Proc Natl Acad Sci U S A. 2021;118(20):e2101100118.
31. Wynn TA, Ramalingam TR. Mechanisms of fibrosis: therapeutic translation for fibrotic disease. Nat Med. 2012;18(7):1028–40.
32. Meng XM, Nikolic-Paterson DJ, Lan HY. TGF-β: the master regulator of fibrosis. Nat Rev Nephrol. 2016;12(6):325–38.
33. Vanaja SK, Russo AJ, Behl B, Banerjee I, Yankova M, Deshmukh SD, Rathinam VAK. Bacterial outer membrane vesicles mediate cytosolic localization of LPS and Caspase-11 activation. Cell. 2016;165(5):1106–19.
34. Murray PJ, Allen JE, Biswas SK, Fisher EA, Gilroy DW, Goerdt S, Gordon S, Hamilton JA, Ivashkiv LB, Lawrence T, Locati M, Mantovani A, Martinez FO, Mege JL, Mosser DM, Natoli G, Saeij JP, Schultze JL, Shirey KA, Sica A, Suttles J, Udalova I, van Ginderachter JA, Vogel SN, Wynn TA. Macrophage activation and polarization: nomenclature and experimental guidelines. Immunity. 2014;41:14–20.
35. Byrne AJ, Maher TM, Lloyd CM. Pulmonary macrophages: a new therapeutic pathway in fibrosing lung disease. Trends Mol Med. 2016;22:303–16.
36. Kishore A, Petrek M. Roles of macrophage polarization and macrophage-derived miRNAs in Pulmonary Fibrosis. Front Immunol. 2021;12:678457.
37. Misharin AV, Morales-Nebreda L, Mutlu GM, Budinger GR, Perlman H. Flow cytometric analysis of macrophages and dendritic cell subsets in the mouse lung. Am J Respir Cell Mol Biol. 2013;49(4):503–10.
38. Kheirollahi V, Wasnick RM, Biasin V, Vazquez-Armendariz AI, Chu X, Moiseenko A, Weiss A, Wilhelm J, Zhang JS, Kwapiszewska G, Herold S, Schermuly RT, Mari B, Li X, Seeger W, Günther A, Bellusci S, El Agha E. Metformin induces lipogenic differentiation in myofibroblasts to reverse lung fibrosis. Nat Commun. 2019;10(1):2987.
39. Tarique AA, Logan J, Thomas E, Holt PG, Sly PD, Fantino E. Phenotypic, functional, and plasticity features of classical and alternatively activated human macrophages. Am J Respir Cell Mol Biol. 2015;53(5):676–88.
40. Ramírez-Hernández AA, Velázquez-Enríquez JM, Santos-Álvarez JC, López-Martínez A, Reyes-Jiménez E, Carrasco-Torres G, González-García K, Vásquez-Garzón VR, Baltierrez-Hoyos R. The role of extracellular vesicles in idiopathic pulmonary fibrosis progression: an approach on their therapeutics potential. Cells. 2022;11:630.
41. Ma JY, Barger MW, Ma JK, Castranova V. Inhibition of respiratory burst activity in alveolar macrophages by bisbenzylisoquinoline alkaloids: characterization of drug-cell interaction. Exp Lung Res. 1992;18(6):829–43.
42. Huang H, Hu G, Wang C, Xu H, Chen X, Qian A. Cepharanthine, an alkaloid from Stephania Cepharantha Hayata, inhibits the inflammatory response in the RAW264.7 cell and mouse models. Inflammation. 2014;37(1):235–46.
43. Vasse GF, Nizamoglu M, Heijink IH, Schlepütz M, van Rijn P, Thomas MJ, Burgess JK, Melgert BN. Macrophage-stroma interactions in fibrosis: biochemical, Biophysical, and Cellular perspectives. J Pathol. 2021;254(4):344–57.
44. He C, Ryan AJ, Murthy S, Carter AB. Accelerated development of pulmonary fibrosis via Cu,Zn-superoxide dismutase-induced alternative activation of macrophages. J Biol Chem. 2013;288(28):20745–57.
45. Redente EF, Keith RC, Janssen W, Henson PM, Ortiz LA, Downey GP, Bratton DL, Riches DW. Tumor necrosis factor-alpha accelerates the resolution of established pulmonary fibrosis in mice by targeting profibrotic lung macrophages. Am J Respir Cell Mol Biol. 2014;50:825–37.
46. Rui Y, Han X, Jiang A, Hu J, Li M, Liu B, Qian F, Huang L. Eucalyptol prevents bleomycin-induced pulmonary fibrosis and M2 macrophage polarization. Eur J Pharmacol. 2022;931:175184.

47. Pushpakom SP, Liptrott NJ, Rodríguez-Nóvoa S, Labarga P, Soriano V, Albalater M, Hopper-Borge E, Bonora S, Di Perri G, Back DJ, Khoo S, Pirmohamed M, Owen A. Genetic variants of ABCC10, a novel tenofovir transporter, are associated with kidney tubular dysfunction. J Infect Dis. 2011;204(1):145–53.
48. Shapouri-Moghaddam A, Mohammadian S, Vazini H, Taghadosi M, Esmaeili SA, Mardani F, Seifi B, Mohammadi A, Afshari JT, Sahebkar A. Macrophage plasticity, polarization, and function in health and disease. J Cell Physiol. 2018;233(9):6425–40.
49. Sakaguchi S, Furusawa S, Wu J, Nagata K. Preventive effects of a biscoclaurine alkaloid, cepharanthine, on endotoxin or tumor necrosis factor-alpha-induced septic shock symptoms: involvement of from cell death in L929 cells and nitric oxide production in raw 264.7 cells. Int Immunopharmacol. 2007;7(2):191–7.
50. Wang J, Xu L, Xiang Z, Ren Y, Zheng X, Zhao Q, Zhou Q, Zhou Y, Xu L, Wang Y. Microcystin-LR ameliorates pulmonary fibrosis via modulating $CD206^{+}$ M2-like macrophage polarization. Cell Death Dis. 2020;11(2):136.

Publisher's note